

Analysis of Wear for a Rocket Sled Slipper

Jun Liu¹, Weihua Wang¹, Feng Zhao¹

¹ Testing Department, Aerospace Life-support Industries Ltd., Xiangyang, China

Abstract. This study analyzed the thermal and stress field of a rocket sled slipper by establishing a thermal-mechanics coupling model. The temperature field and thermal stress field were obtained. The results are compared with real rocket sled run test. It shows that there is an agreement of wear distance between the test and simulation. However, the real test local temperature which is above 1470 °C, in evidence of detected Cristobalite-high SiO₂, is much higher than simulation result which is 818 °C, due to high vibration impact load in real run test.

1. Introduction

Rocket sled tests are ground test platforms which enables equipment to be tested under high acceleration or high airspeed conditions. Such working condition can cause slipper wear[1].

In the study of material wear characteristic, temperature and stress are the two most important coupling parameters. Temperature rise caused by friction is a complicated nonlinear physical process. During the test, the work done by friction is converted to heat and passes into the contact area of the slippers, which increases the temperature of the slipper and produces thermal stress. The temperature rises as the rocket sled flies, resulting in change of material performance and thermal stress, influencing on boundary conditions of temperature field and stress field distribution. At present, numerical methods are generally used for the study of plane sliding friction[2].

This study aims to establish a finite element structure and thermal coupling model to obtain the temperature and stress distribution of the slipper, and compare the results with real run test..

2. Theory

2.1. Basics

In the process of friction, the frictional energy caused by deformation or destruction in contact surface material convert into thermal energy, and thus the surface temperature of the friction material is raised. When under high flying velocity, strong friction heat generated in the contact surface changing the state of the contact surface, leading to the material performance change and thereby failure in meeting the demand of actual working condition. For example, thermal stress can change the contact surface conditions; thermal expansion can change the initial parts fit etc. At the same time, the thermal stress produced by friction heat has an effect on the overall stress distribution. Therefore, it is necessary to conduct temperature analysis first. In the run test, the maximum working speed of the rocket sled can reach 2.8 Ma, therefore the slippers will cause detached shock wave, which will heat the windward side, and other surfaces are also heated due to aerodynamic heating effect. But since the overall operation time is not greater than 8s, the aerodynamic heating effect is not obvious. To facilitate the calculation, the simulation model is based on the following assumptions.

- a) The heat removed by grinding and peeling is ignored;



- b) The aerodynamic heat effect caused by the detached shock wave is ignored.
- c) The aerodynamic heat effect of the slipper surface is ignored, and the surrounding fluid temperature is considered as the local temperature.
- d) The materials are isotropic.

2.2. Heat conduction equation in finite element

In the process of plane sliding friction, the main heat transfer is the heat conduction between the contact surfaces and the heat convection between the object and the surrounding air. In the calculation of temperature, the basic equation is equation 1,

$$\rho c \frac{\partial T}{\partial \tau} = \left[\frac{\partial}{\partial x} \left(\lambda \frac{\partial T}{\partial x} \right) + \frac{\partial}{\partial y} \left(\lambda \frac{\partial T}{\partial y} \right) + \frac{\partial}{\partial z} \left(\lambda \frac{\partial T}{\partial z} \right) \right] + q \quad (1)$$

where q is the heat generates inside particle $dxdydz$, τ is the temperature rise in particle.

The equation can be simplified as equation 2 when there is no interior heat source and the coefficient of thermal conductivity of material is not changed with position.

$$\frac{\rho c}{\lambda} \frac{\partial T}{\partial \tau} = \frac{\partial^2 T}{\partial x^2} + \frac{\partial^2 T}{\partial y^2} + \frac{\partial^2 T}{\partial z^2} \quad (2)$$

2.3. Calculation of heat flux density

According to the heat transfer theory, the friction heat generated by plane friction is distributed between two contact objects following the following principles:

Friction heat between two different materials is not evenly distributed to two contact surfaces, and the distribution relationship is always related to the thermal properties of materials. The generation and distribution of frictional heat can be seen as such there is a continuous exothermic plane transient heat source in between, and the heat transfer can be seen as the superposition of the transient heat source. For rocket sled slippers, the friction heat entering the contact surface of the slipper is equation 3,

$$q_1 = \frac{k}{1+k} \mu \cdot N \cdot v \quad (3)$$

where q is total heat flux, N is load on slipper, v is velocity, k is coefficient of heat partition.

2.4. 2.4 Stress analysis

In rocket sled run, the friction heat continuously enters slippers from the contact surface, making the slipper temperature rise continuously. The thermal stress can be calculated according to equation 4,

$$[\sigma] = \Delta T \cdot [\alpha(T)] \quad (4)$$

In finite element analysis, the thermal load can be considered as equivalent to force applied on the corresponding node. According to the theory of thermal stress, the stress analysis constitutive equation under thermal stress is equation 5,

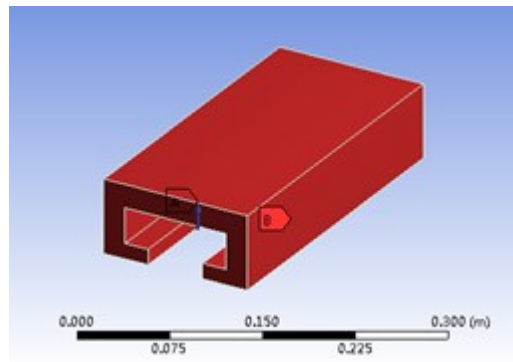
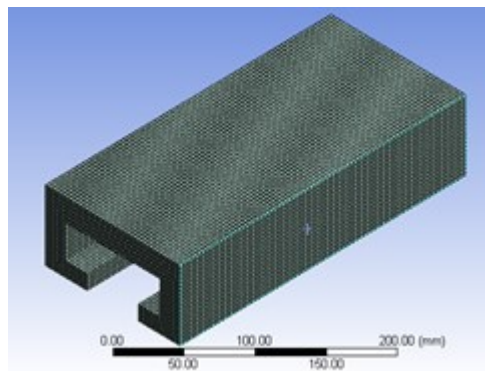
$$[\sigma] = [D] \cdot ([\varepsilon] - \Delta T \cdot [\alpha(T)]) \quad (5)$$

where $[\sigma]$ is stress matrix, $[D]$ is stiffness matrix, $[\varepsilon]$ is strain matrix, ΔT is temperature variable, $[\alpha(T)]$ is coefficient of linear expansion.

3. Simulation

3.1. Geometry and Model

The 3D geometry was built in ANSYS shown in Figure 1. 3mm hexahedral elements are applied in mesh shown in Figure 2. The material properties and conditions are listed in Table 1 and Table 2.

**Figure 1.** Geometry model**Figure 2.** View of mesh**Table 1.** Ial properties and condition parameters.

Parameters	Value
Load	2000N
Contact size	94mm×284mm
Maximum speed	750m/s
Slipper thickness	21mm
Acceleration	$93.75\text{m}\cdot\text{s}^{-2}$
Operating time	8s

Table 2. Al parameters of slipper and track.

Object	Temperat ure (°C)	Special heat J/(g·°C))	Thermal conductiv ity J/(mm·s·° C)	Density ρ (g/cm ³)
Slipper 0Cr18Ni9Ti	20	0.462	0.0146	7.75
	200	0.512	0.0161	
	400	0.540	0.0180	
	800	0.604	0.0239	
Track U71Mn	20	0.472	0.147	7.92
	200	0.480	0.143	
	400	0.524	0.138	
	800	0.615	0.132	

3.2. Boundary Conditions

The boundary conditions for the model to solve finite element heat transfer equation and stress equation are stated as following.

- a) The friction contact surface of slipper applies the second boundary condition. The heat flux density is calculated according to the equation 3 and thus yields the second boundary condition;
- b) All surfaces except the contact surfaces apply the first boundary condition, and the surface temperature is the ambient temperature;
- c) Normal pressure load is exerted on the surface of slipper.
- d) Fixed support is applied on slipper contact surface. A, B, C, and D points apply constraints on z-axis and freedom on X and Y axis.

3.3. Simulation result

The temperature distribution is shown in Figure 3. The curves of contact surface temperature and maximum stress varying with time respectively are illustrated in Figure 4.

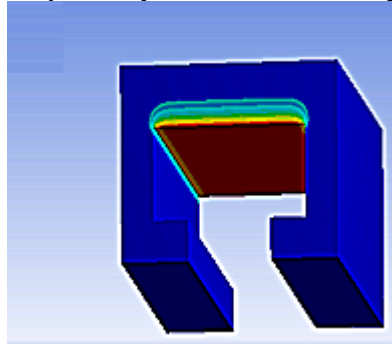


Figure 3. Temperature distribution

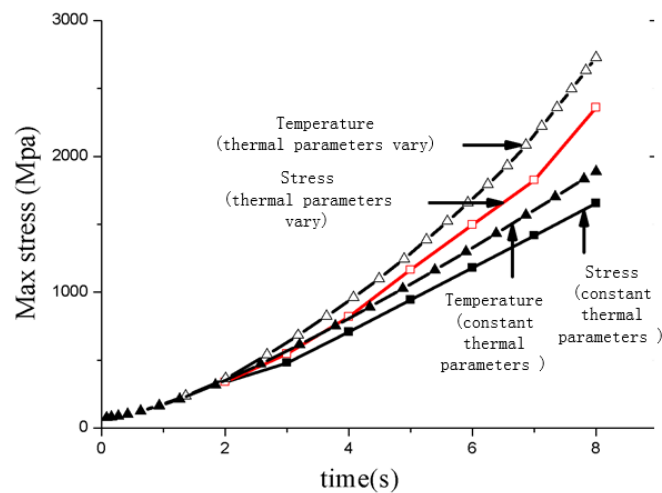


Figure 4. Contact surface temperature varies with time ; Maximum stress varies with time

From the contact surface temperature, it can be seen that, over time, friction heat flow continuously enters into the contact surface, making contact surface temperature rise[3]. The solution of the maximum temperature can reach 818 °C, the maximum temperature located on friction contact surface. The maximum stress is 2350 MPa which can be read from Figure 4.

The solution of temperature distribution was transfer into load and solved in stress field. The result observed from Figure 5 shows that the maximum stress is also located on the contact surface and the stress and strain in friction heat response area are much higher than other areas.

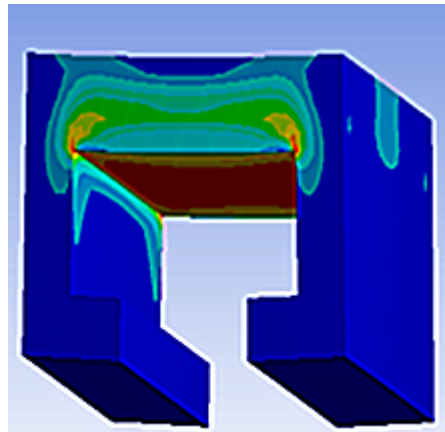


Figure 5. Stress field distribution

The variations of the total strain and thermal stress along a certain direction were mapped in Figure 6. Figure 7 shows the variations of the total strain and thermal strain along a certain direction. From the graphs, it can be seen that the temperature is high and changes dramatically within 6 mm distance from the contact interface, and the thermal strain is the dominate strain source. In the range of 6mm to 14mm distance from the interface, the difference between the strain due to thermal and the strain due to contact load are small. The thermal strain varies slowly and the load stress is the dominant influencing factor. From 14mm to the top surface of the slipper, the thermal strain does not change evidently. The strain due to load is the dominant factor and the total strain increases. The area within 6 mm from the interface is the thermal concentrated zone and has the highest strain.

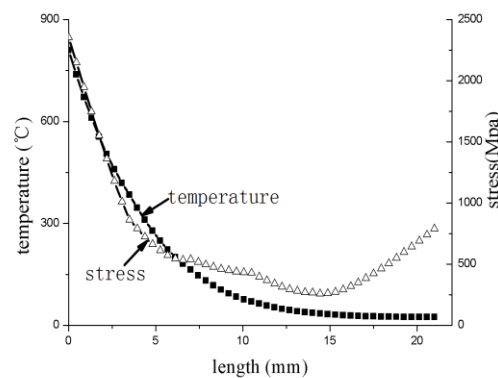


Figure 6. The variations of the temperature and stress along a certain direction

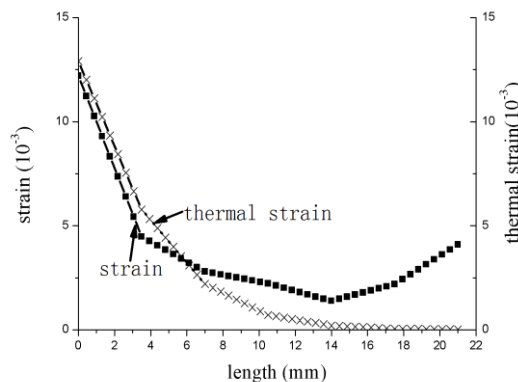


Figure 7. The variations of the total strain and thermal strain along a certain direction

4. Experiment analysis

4.1. Observation of slippers

In real test, 6 mm plates were installed on the corresponding locations on the slipper surface. The positions relative to the track are shown in Figure 8 a. An analysis was conducted on the macro morphology of the slipper. The slipper plate samples were taken from a rocket sled after run test. The overview of worn samples is shown in Figure 8 b-f.

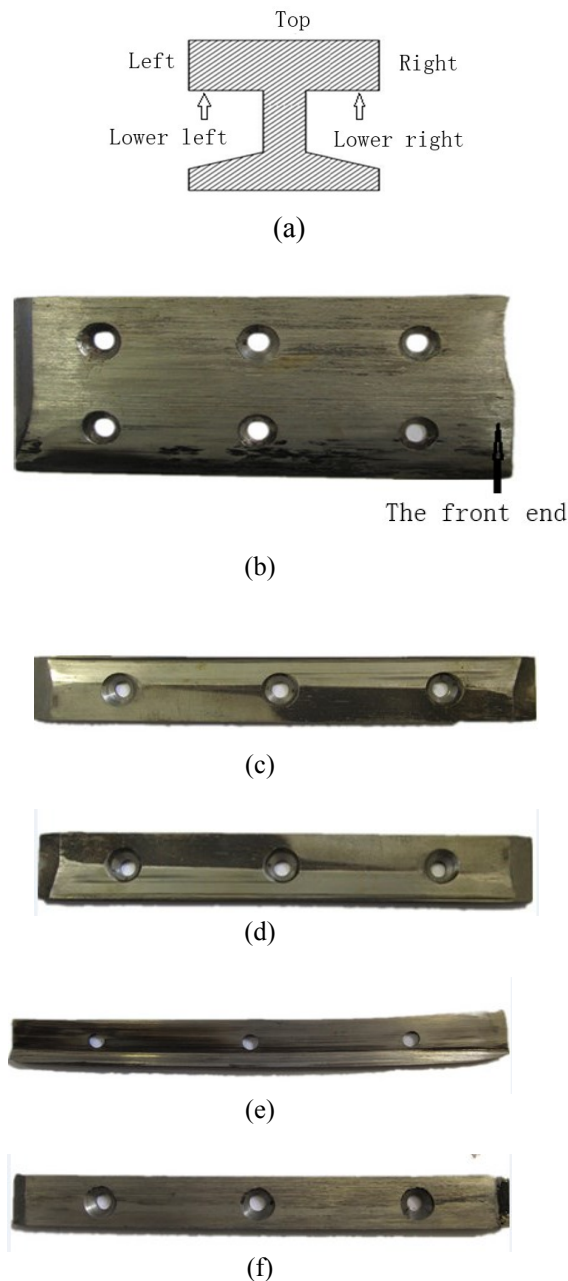


Figure 8. Sample photos

(a. Schematic of slipper plate positions b. Top slipper plate c. Left slipper plate d. Right slipper plate e. Lower left slipper plate f. Lower right slipper plate)

The changes of slipper dimensions were measured in Table 3.

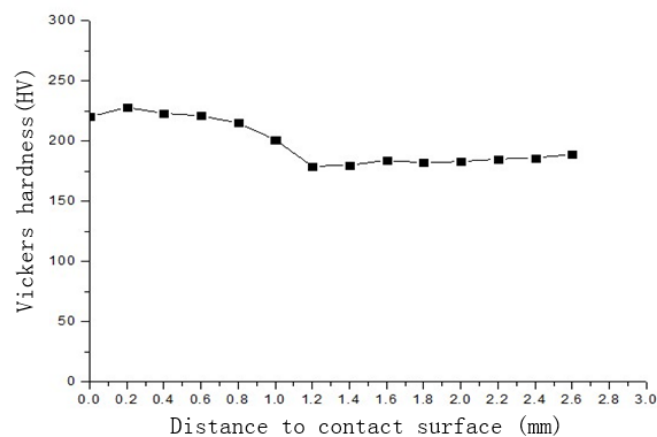
Table 3. Al parameters of slipper and track.

Position	Front /mm	Middle /mm	Rear /mm	Original /mm
Top	2.7	5.6	5.8	6
Left	5.1	6	6	
Right	4.9	5.8	5.6	
Lower left	1.2	1.2	1.9	
Lower right	5.5	5.5	5.6	

From Table III it can be seen that the front and lower left slipper were seriously worn. The front end of top slipper was worn into sharp shape. The lower left slipper was highly deformed compared to original shape. The total thickness changed obviously. No obvious thickness changes were observed from other slippers.

4.2. Hardness test on slippers

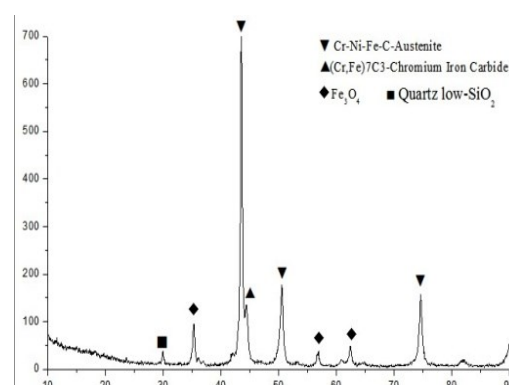
The samples were analyzed by hardness tester TY10MH-5. The samples were cut into 20mm×20mm×3mm specimens. Hardness was tested every 0.2mm in thickness direction. The results are illustrated in Figure 8.

**Figure 9.** Hardness test results on vertical cross section

It is obvious that the surface hardness is obviously higher than the interior base. It confirms that the wear behavior resulted in plastic deformation and thereby work hardening.

4.3. Wear surface product analysis

The specimens were analyzed by X-ray diffractometer. The results are shown in Figure 10.



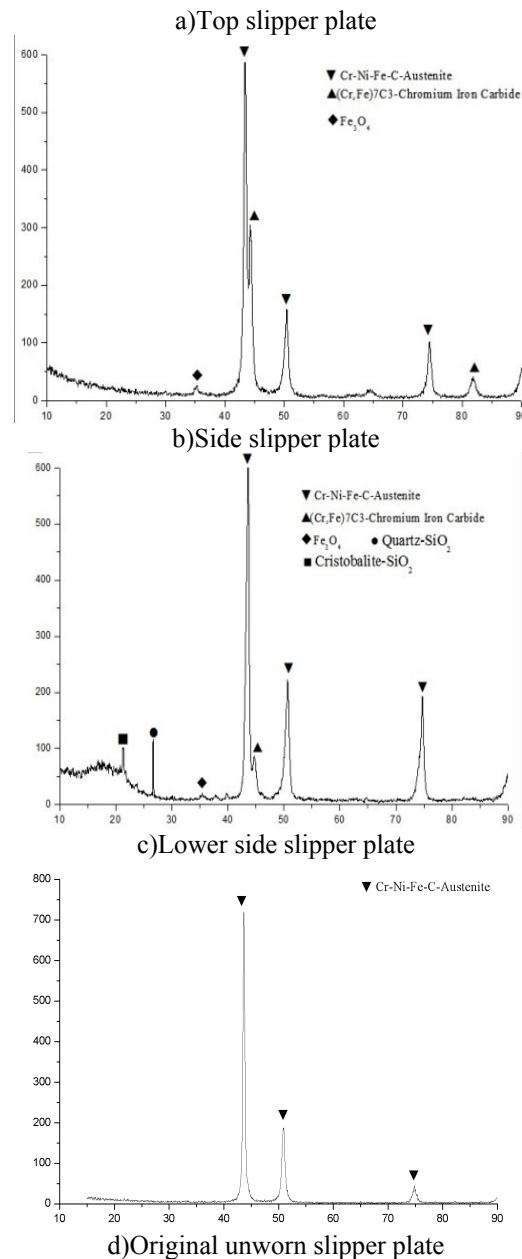
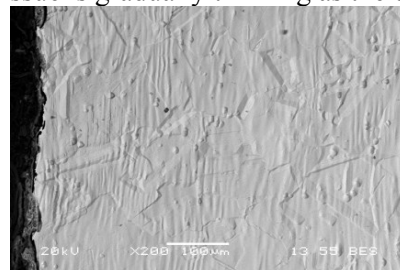


Figure 10. XRD analysis on failure and original samples

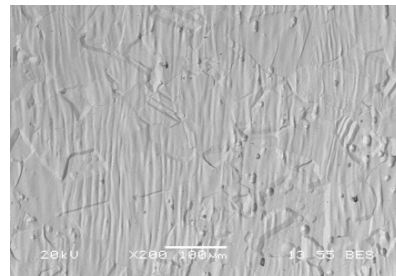
From Figure 10 d) we know that there is only austenite microstructure in original slipper. After run, Fe_3O_4 and $(\text{Cr}, \text{Fe})_7\text{C}_3$ can be observed on the surfaces. It can be inferred that the temperature reaches 650°C between the contact pairs. Furthermore, Cristobalite-high SiO_2 was detected on the lower left slipper, which indicates that the temperature of surface area was above 1470°C . Since Si was not existed in the slipper material, the compound is believed to be generated due to the mix of impurities in the air. In addition, the rocket sled is believed to be under an abnormal attitude leading a high loading condition and high friction heat was generated on the lower left side slipper. Because of severe vibration load in real test causing high impact load, the surface temperature is higher than the simulation result.

4.4. Observation of microstructure

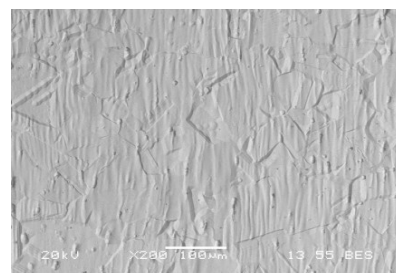
Figure 11 shows typical microtopography of top and side slipper plates. Obvious difference can be seen along the vertical direction starting from the contact surface[4]. Heat-stress coupled tissue can be observed in the area of contact surface and contiguous zone, where there can't see obvious grain, and is uneven. The surface shows a stairway shape, and there are cracks in the dense tissue of the surface layer. The thermal-stress coupled issue is gradually thinning as the distance from surface increases.



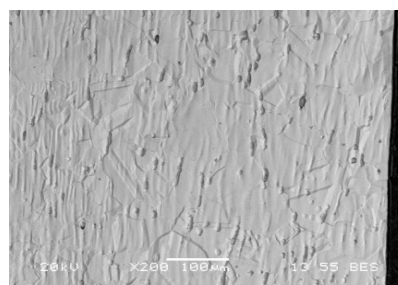
(a)



(b)



(c)



(d)

Figure 11. Typical Microscopic microstructure of samples

5. Conclusion

Simulation and Experiment results conducted in this work allowed the following conclusion:

For a rocket sled run of speed 750m/s and time of 8 seconds simulation, the maximum temperature reaches 818°C, the maximum stress is 2350 MPa. The friction heat and stress are concentrated within 6 mm distance from contact surface. In contrast, the analysis of macro morphology of the slipper taken from real run test shows that local temperature reaches 1470 °C under this speed and time condition in

evidence of Cristobalite-high SiO₂ generated. The worn distance is in good agreement with simulation result. Under the double action of vertical impact load and frictional heat, thermal-stress coupling tissues in the material are produced proved by microstructure observation.

The temperature difference is mainly because that the simulation applies an idealistic condition that not taking account of the vibration load, and impurities in the air environment combining the materials generate Cristobalite-high SiO₂ in high temperature.

6. References

- [1] Cameron G. J 2007 An Evaluation of High Velocity Wear, AFIT/GAE/ENY/07-M06. Master's thesis, Air Force Institute of Technology *J. Wright Patterson AFB, OH* **2** 07.
- [2] Cameron G and Palazotto A 2008 An Evaluation of High Velocity Wear *J. Elissa, "Title of paper if known, " unpublished* **7** 1066-1075
- [3] Stephen P 2010 Consideration of Wear at High Velocities, AFIT/GAE/ENY/10-M16. Master's thesis *J. Air Force Institute of Technology, Wright Patterson AFB, OH* **24** 18
- [4] Tachau R D M, Yew C H and Trucano T G 1995 Gouge initiation in high-velocity rocket sled testing *J. International journal of impact engineering* **4** 825-836